AJNR

Experimental brain abscess: enhanced sonography and pathologic correlation.

D R Enzmann, B E Lyons, B Carroll, R C Placone, J Rasor, R H Britt, J Buxton and D Wilson

AJNR Am J Neuroradiol 1982, 3 (1) 41-45
http://www.ajnr.org/content/3/1/41

Experimental Brain Abscess: Enhanced Sonography and Pathologic Correlation

D. R. Enzmann[1]
B. E. Lyons[1]
B. Carroll[1]
R. C. Placone[1]
J. Rasor[2]
R. H. Britt[3]
J. Buxton[4]
D. Wilson[4]

A new sonographic contrast agent, gelatin-encapsulated nitrogen microbubbles, was introduced intraarterially to enhance the high-resolution sonographic scan of an experimental brain abscess. The echogenicity produced by the microbubbles correlated closely to the site and distribution of abscess neovascularity. The contrast agent aided in the detection of small necrotic centers in the late stages of abscess evolution when these centers were not visualized on noncontrast sonograms. The echogenic effect of the microbubbles was maximum immediately after injection; it decreased by 5 min and had virtually disappeared at 15 min.

Echoencephalography has received renewed attention with the development of high-resolution B scanners, but its neuroradiologic application requires improved understanding of the sonographic imaging properties of brain abnormalities. Correlation of high-resolution scans, computed tomographic (CT) scans, and neuropathologic findings can provide such basic information [1]. High-resolution scanning has also stimulated research in sonographic contrast agents with some encouraging results [2, 3]. We report our experience with intravascular gelatin-encapsulated microbubbles (GEM) in an experimental brain abscess model to refine our knowledge of its pathogenesis and sonographic imaging properties.

Materials and Methods

In three mongrel dogs, brain abscesses were produced with alpha streptococcus (10^8–10^9 colony-forming units) using a previously described technique [4].

High Resolution Sonograms

Coronal and sagittal high resolution sonograms were obtained through scalp musculature over a large craniotomy defect immediately after surgery to document the initial appearance of the injected agar-broth mixture. Subsequently, precontrast and dynamic, real-time postcontrast scans were obtained during the late cerebritis stage, day 6, and during the late capsule stage, day 15 or day 16, in each dog.

The sonographic imaging system (SRI International) was a real-time B scanner using a 10 MHz, 64 element, linear array. Dynamic focusing was used in both transmit and receive to provide submillimeter resolution in both dimensions over the entire image. A fixed acoustical lens provided focusing in the direction orthogonal to the image plane. The field of view was 3 × 4 cm and images were generated at 30 frames/sec.

Gelatin-encapsulated nitrogen microbubbles (GEM) were used as a contrast agent in conjunction with dynamic scanning. To prevent motion, the dog's head was affixed to a stereotactic device and the transducer was immobilized over the region of interest using a ring stand and clamps. Gelatin-encapsulated nitrogen microbubbles were administered intraarterially through a 5 French polyethylene catheter placed selectively in the carotid artery ipsilateral to the abscess. One cc of 25 μm spectrum GEMs was injected by hand over a period of 8–12 sec. Each cc contained 2–6 × 10^7 microbubbles, the size of which

Received June 9, 1981; accepted after revision August 10, 1981.

This work was supported by National Institutes of Health grant 5RO1 NS16404-01.

[1] Department of Radiology, Stanford University Medical Center, Stanford, CA 94305. Address reprint requests to D. R. Enzmann.

[2] Rasor Associates, Inc., Sunnyvale, CA 94086.

[3] Division of Neurosurgery, Stanford University School of Medicine, Stanford, CA 94305.

[4] SRI International, Menlo Park, CA 94025.

***AJNR* 3:41–45, January/February 1982**
0195-6108/82/0301-0041 $00.00

ranged from 1 to 50 μm. Distribution of these microbubbles was as follows: 0–10 μm, 9%; 11–20 μm, 34%; 21–30 μm, 17%; 31–40 μm, 28%; and 41–50 μm, 12%. The mean microbubble size was 25 ± 12 μm. Glycerol was used as the injection vehicle. Dynamic imaging of the microbubble wash-in phase was accomplished by continuous videotape recording starting with a precontrast baseline view extending through the injection phase and continuing to the first evidence of decreasing contrast effect. Images at 1 sec intervals were selected from the videotape, transferred to video disk, and then photographed on a multiformat camera. Intermittent videotape recording and Polaroid images were obtained 5, 10, and 15 min after injection to document the washout phase.

Neuropathologic Evaluation

Neuropathologic evaluation of the experimental brain abscess was accomplished by sacrificing the dogs immediately after the late capsule imaging study (day 15 or 16). The dog's entire brain was removed and placed in 10% formalin for at least 5 weeks. The brain was then cut into 0.5 cm coronal slices and photographed for comparison with the sonogram. Sections encompassing the entire abscess were cut and processed and stained with the following stains: hematoxylin and eosin for general cytologic features, Gram stain for bacteria, reticulin stain for reticulin or precollagen, Masson trichrome and hematoxylin van Gieson for mature collagen, and Mallory phosphotungstic acid (PTAH) and glial fibrillary acid protein (GFAP) stains for gliosis and reactive astrocytosis.

Results

Sonography was limited to the late cerebritis stage (day 6) and the late capsule stage (day 15 or 16). In the cerebritis stage, the abscess was characterized by an echogenic rim surrounding a hypoechoic center (figs. 1 and 2). The thickness of the hyperechoic rim varied from lesion to lesion (3–6 mm), but was relatively uniform compared with the late capsule stage for the same lesion. No neuropathologic correlation was available for this stage of abscess formation in this study. One of the three abscesses had a multiloculated appearance, that is, two adjacent hyperechoic rims, in the cerebritis stage. This lesion was subsequently shown both by the sonogram and neuropathologic examination to retain these multilocular features in the late capsule stage (fig. 3).

In the cerebritis stage, the intraarterial injection of microbubbles produced scattered areas of increased echogenicity, which appeared rapidly as the microbubbles lodged in vessels. Deposition of microbubbles occurred primarily in the echogenic rim with a greater number on the cortical aspect of the abscess compared with the ventricular side (figs. 1 and 2). Some microbubble deposition occurred along the external border of the precontrast echogenic rim resulting in a thickened rim (figs. 1 and 2). Real-time videotape images obtained during the wash-in phase revealed microbubbles traversing the hypoechoic center demonstrating the presence of intact vessels. Only a few new echoes were identified within the hypoechoic center (fig. 1). The increase in echogenicity of the lesion as a whole was not marked when compared with the change observed in the late capsule stage.

In the late capsule stage on the precontrast scan, the lesion was significantly smaller compared with the cerebritis stage. The echogenic rim had increased in thickness and the hypoechoic center had decreased in size or become undetectable. Both the inner and outer edges of the echogenic rim were more irregular. Neuropathologically, this was explained by extensive collagen deposition around proliferating neovascularity that extended both into the necrotic center and into surrounding brain (figs. 4–6). When the necrotic center was undetectable, it was obscured by echoes produced by the inhomogeneity of its histologic features (fig. 6). A well localized necrotic center, which was occupied by a relatively homogeneous sea of polymorphonuclear leukocytes, was also obscured by low-level echoes on the precontrast scan (fig. 7).

The intraarterial injection of microbubbles in the late capsule stage caused a marked increase of echogenicity of the abscess compared with the precontrast scan (fig. 8). The overall increase in echogenicity of the abscess was markedly greater in the capsule stage (fig. 8) than in the cerebritis stage (figs. 1 and 2). This increase occurred in areas that were already echogenic on the precontrast scan. As in the cerebritis stage, these increased echoes appeared immediately during the wash-in phase of the microbubble injection. In the capsule stage, precontrast scan echogenicity correlated best with the distribution of perivascular collagen deposition. Since the microbubbles were intravascular, their distribution correlated closely to the neuropathologic localization of vessels diffusely throughout the lesion, but particularly intense around residual necrotic centers. The echogenicity around the centers was enhanced with microbubbles, even if the residual center was quite small. The multilocular character of the resolving necrotic center in these late stages could only be appreciated with GEM (fig. 8).

Maximum echo enhancement was detected immediately after the wash-in phase of the intraarterial injection of microbubbles for both the cerebritis and capsule stages (fig. 9). This augmentation of echogenicity remained stable for several minutes but began to decrease by 5 min. At 10 min after injection, most of the GEM had dissolved with only a few areas still showing augmented echoes. The microbubble effect had essentially disappeared 15 min after injection. Although the dogs were under sedation, no side effects were noted during or after the injection of microbubbles. No microscopic evidence of microbubble damage was noted; however, the extensive changes produced by the abscess itself precluded any sensitive measure of structural injury.

Discussion

Gelatin-encapsulated microbubbles are a significant departure from contrast agents usually used in radiologic examinations. GEM are intravascular agents distinct from the more common radiographic water-soluble iodinated compounds, which, although intravascular for a short period, are primarily extravascular contrast agents. By virtue of their size, microbubbles are restricted to the intravascular space. They are excellent sonographic contrast agents; only

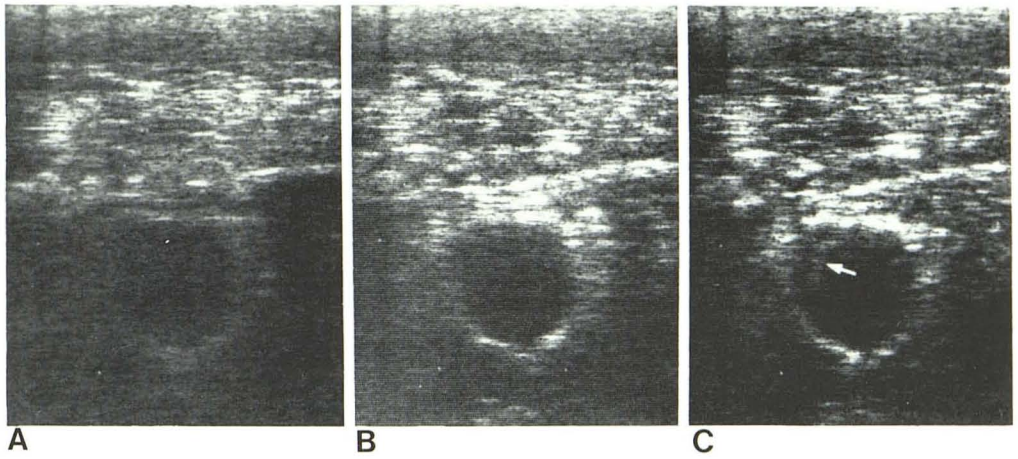

Fig. 1.—Serial sagittal high-resolution sonograms of day 6 brain abscess before (**A**) and 3 (**B**) and 9 sec (**C**) after intracarotid injection of GEM. **A**, Precontrast scan. Thin echogenic rim surrounds hypoechoic center typical of cerebritis stage. Horizontal echoes in upper half of image represent scalp musculature and dura. **B**, Early wash-in phase. Increased echogenicity within rim, more on cortical aspect of abscess. Echoes around rim were also more echogenic than in **A**. **C**, Late wash-in phase. Further augmentation of echoes in rim with continued predominance on cortical side. Small area of echogenicity within hypoechoic center (*arrow*) corresponds to known areas of neovascularity in this model.

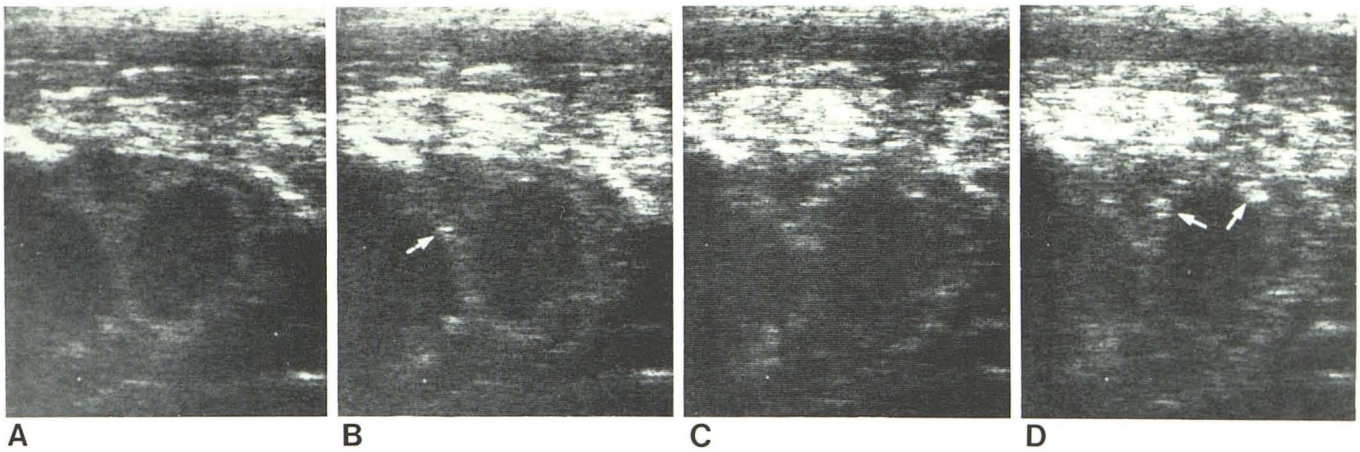

Fig. 2.—Serial sagittal high-resolution sonograms of day 6 brain abscess before (**A**) and 3 (**B**), 6 (**C**), and 11 (**D**) sec after intracarotid injection of GEM. **A**, Noncontrast scan. Two adjacent echogenic rims, each with hypoechoic centers. Surrounding brain is hypoechoic except for cortical sulcus (oblique line of echoes) on superior lateral aspect of right lesion. **B**, Early wash-in phase. Only scattered areas of increased echogenicity (*arrow*). **C**, 6 sec. Echogenic rims appear thicker, especially on cortical aspect. **D**, Late wash-in phase. Further deposition of GEM (*arrows*). In **A**, peripheral areas were hypoechoic. Overall magnitude of echo augmentation was relatively low compared with later capsule stage (fig. 8).

small volumes of microbubbles result in marked changes in intravascular acoustic impedance, producing increased echogenicity [2, 3]. The GEM used in this study would be expected to lodge in small arterioles and capillaries and thus identify this arterial anatomy in the experimental brain abscess. Portrayal of vascularity by the microbubbles correlated closely with neuropathologic findings. Although inflammatory neovascularity in the brain differs from normal brain vasculature, it appeared that the deposition of microbubbles correlated best with the amount of vascularity rather than any particular characteristic of this neovascularity. The echo augmentation produced by microbubbles was similar to that observed in an experimental tumor model [3].

In the cerebritis stage of abscess formation, an echogenic rim around a hypoechoic center characterized the high-resolution sonogram. The rim represented the marked cellular infiltrate around the developing necrotic center [1]. Intraarterial injection of microbubbles at this stage resulted in only a minimal increase in the echogenicity of this rim, suggesting that the rim was relatively hypovascular. The echogenic enhancement was located primarily on the cortical aspect of developing abscess, reflecting the more rapid development of neovascularity at this site [1, 4]. This has been confirmed neuropathologically [1, 4]. Early neovascularity, which lacked significant perivascular collagen, was not echogenic on the noncontrast scan, but accumulation of microbubbles within these vessels allowed their identification peripheral to the cellular infiltrate, as evidenced by thickening of the echogenic rim (figs. 1 and 2). Although the echogenicity of the necrotic center was minimally increased by microbubbles, real-time videotape viewing showed them moving through the necrotic center, indicating the presence of intact vessels. This finding and that of delayed contrast enhancement on the CT indicate the presence of some central vascularity in the cerebritis stage [1, 4].

In the capsule stage of abscess evolution, the noncontrast

3

4

Fig. 3.—Day 15 of encapsulated abscess in figs. 7–9. Two separate necrotic centers were identified, each surrounded by thick collagen capsule. Low power view shows irregular outer border of capsule with extensions of collagen penetrating into surrounding brain. One necrotic center (left) was inhomogeneous collection of liquid debris and cellular infiltrate, while second (right) consisted of more uniform collection of polymorphonuclear neutrophils. Both types of necrotic centers were echogenic (Cf. fig. 8). (Trichrome ×11.)

Fig. 4.—Day 16 of encapsulated brain abscess. Low power view shows well developed collagen capsule around inhomogeneous necrotic center. Echogenic rim on scan correlated with distribution of collagen fibers, while hypoechoic center represented necrotic center. However, as in this specimen, inhomogeneity of necrotic center could result in echogenicity with resultant obscuration of boundaries on noncontrast scan. (Trichrome, ×11.)

5

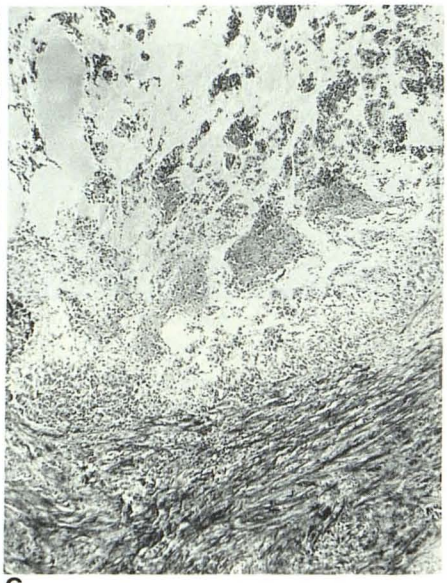

6

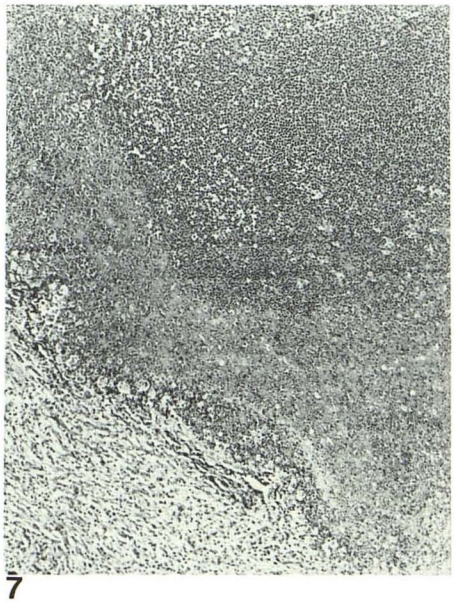

7

Fig. 5.—Junction between outside border of collagen capsule and surrounding brain. Outer collagen fibers, deposited primarily in perivascular distribution, have more irregular appearance compared with more centrally located concentric fibers. Numerous macrophages intermingled with collagen fibers. Irregular interface between outside collagen capsule and surrounding brain corresponds to poorly circumscribed outside border of echogenic rim. (Trichrome, ×75).

Fig. 6.—Inner border between necrotic center (top) and collagen capsule. Necrotic center composed of primarily liquefied debris with scattered islands of inflammatory cells. These islands of cells produce echoes when large. The most central part of collagen capsule showed characteristic concentric deposition of fibers. (Trichrome, ×75.)

Fig. 7.—Necrotic center (bottom) is a sea of acute inflammatory cells. Little liquefied material is present. This type of necrotic center produced low-level homogeneous echo pattern. Distribution of microbubbles around necrotic center allowed its identification. Collagen fibers (lower left) of capsule were present but relatively poorly formed in this part of abscess. (Trichrome, ×75.)

scan showed a smaller lesion with a thicker, more irregular echogenic rim around a smaller hypoechoic center [1]. At times, a definite hypoechoic region could not be identified; rather, the entire lesion consisted of low-level echoes. Echoes in the necrotic center were caused by inhomogeneous pockets of inflammatory cells and liquid debris. The injection of microbubbles caused a marked increase in echoes throughout the entire abscess, except the necrotic center. Small necrotic centers were now readily visualized as hypoechoic because they were surrounded by marked echogenicity. Even in retrospect, these small necrotic centers were not identifiable on the noncontrast scan. The difference in accumulation and distribution of microbubbles in the cerebritis and capsule stages reflected the quantita-

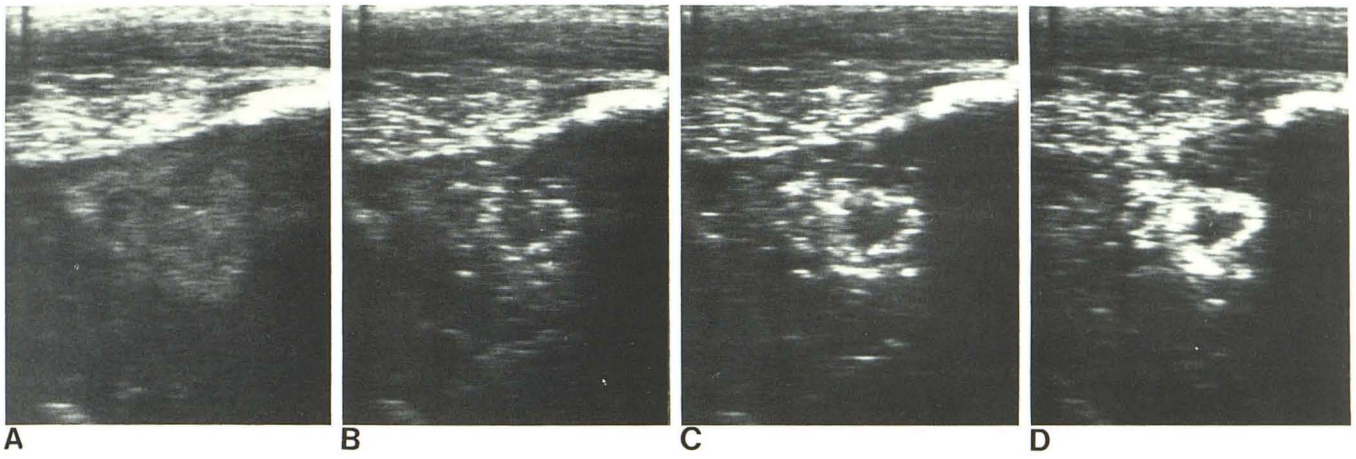

Fig. 8.—Serial sagittal high resolution sonograms of day 15 brain abscess before (**A**) and 2 (**B**), 4 (**C**), and 6 (**D**) sec after intracarotid injection of GEM (later version of lesion in fig. 2). Its size had decreased but it retained its multiloculated character, although this was not appreciated on **A**, which showed relatively solid area of echoes. Scattered peripheral echoes represented perivascular collagen deposition around main capsule. **B–D**, Wash-in phase. Progressive deposition of microbubbles result in marked increase in echogenicity of lesion. These new echoes have formed two thick echogenic rings, corresponding to neuropathologic loculations in fig. 2. Pathologically, site of microbubble deposition correlated best with vessels in well developed collagen capsule. Relatively hypoechoic centers on postcontrast scan represented necrotic centers. Echo augmentation was much greater in capsule stage compared with cerebritis stage in same abscess (fig. 2).

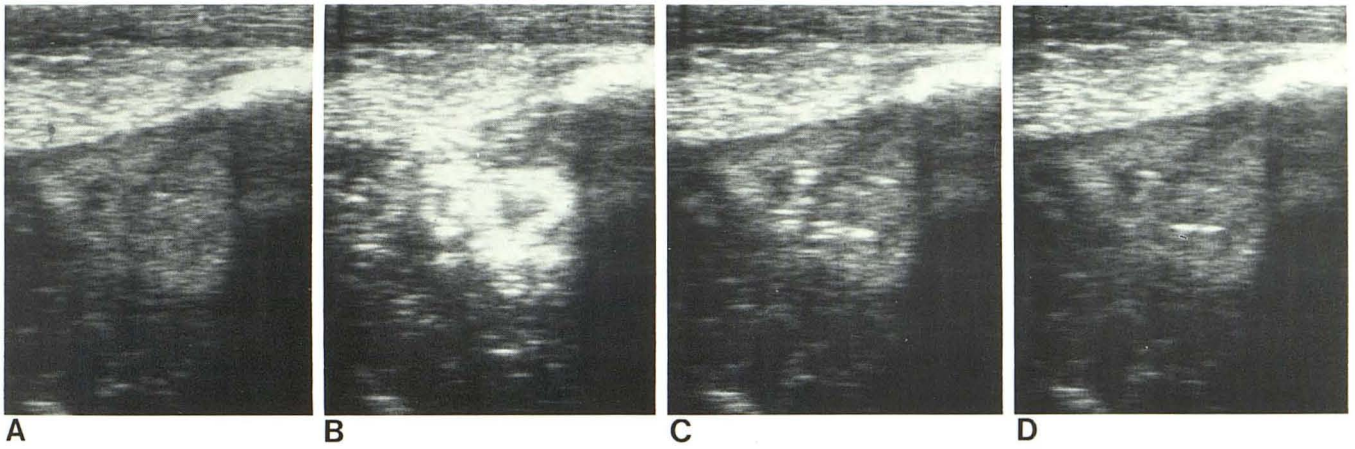

Fig. 9.—Serial sagittal high-resolution sonograms of day 15 brain abscess; washout or dissolution phase of GEM. **A**, Noncontrast scan. Lesion composed of relatively homogeneous echoes surrounded by scattered echoes. **B**, Immediately after injection of GEM. Marked increase in echogenicity, with two small residual necrotic centers becoming detectable. **C**, Microbubbles rapidly dissolved, resulting in decreased echogenicity by 5 min. **D**, near absence of enhancement effect by 10 min.

tive difference in vascularity of these abscess stages.

Gelatin-encapsulated microbubbles proved to be an excellent sonographic intravascular contrast agent. The distribution of these microbubbles correlated closely to the time course of development and the localization of neovascularity in this experimental brain abscess model. With appropriate calibration, qualitative and possibly quantitative estimates of blood flow seem possible. Although introduction is currently limited to intraarterial injection, further investigation of this contrast agent could prove fruitful in furthering both the imaging and quantitative potential of high-resolution sonography.

REFERENCES

1. Enzmann DR, Britt RH, Lyons B, Carroll B, Wilson DA, Buxton J. High resolution ultrasound evaluation of experimental brain abscess evolution: comparison with CT and neuropathology. *Radiology* **1982** (In press.)
2. Meltzer RS, Tickner EG, Sahines TP, Popp RL. The source of ultrasound contrast effect. *JCU* **1980**;8:121–127
3. Carroll BA, Turner RJ, Tuckner EG, Boyle DB, Young SW. Gelatin encapsulated nitrogen microbubbles as ultrasonic contrast agents. *Invest Radiol* **1980**;15:260–266
4. Enzmann DR, Britt RH, Yeager AS. Experimental brain abscess evolution: computed tomographic and neuropathologic correlation. *Radiology* **1979**;133:113–122